Deciphering the role of monosaccharides during phage infection of Staphylococcus aureus

Baptiste Arbez, Marion Gardette, Christophe Gantzer, Neus Vilà, Isabelle Bertrand, Sofiane El-Kirat-Chatel

GRAPHICAL TABLE OF CONTENTS

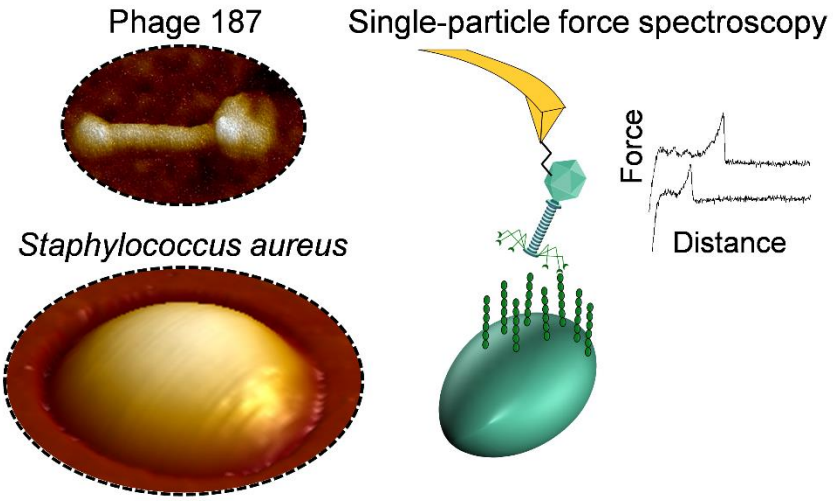

Graphical table of contents. *S. aureus* cell wall was deciphered using a phage-decorated atomic force spectroscopy tip in order to identify major receptors involved in phage adhesion and infection of host cell.

Deciphering the role of monosaccharides during phage infection of *Staphylococcus aureus*.

Baptiste Arbez[a], Marion Gardette[a], Christophe Gantzer[a], Neus Vilà[a], Isabelle Bertrand[a] and Sofiane El-Kirat-Chatel[a]*

[a] Laboratoire de Chimie Physique et Microbiologie pour les Matériaux et l'Environnement (LCPME), CNRS, Université de Lorraine, 405 rue de Vandoeuvre, 54602 Villers-lès-Nancy France

*Address correspondence to Sofiane El-Kirat-Chatel: elkirat1@univ-lorraine.fr

ABSTRACT

As phages are extensively investigated as novel therapy tools but also as transfer agents for antibiotic resistance genes, thorough understanding of phage-host interactions becomes crucial. Prerequisite for phage infection is its adhesion to the host surface. Here, we used atomic force microscopy-based single-particle force spectroscopy with phage-decorated tips to decipher the adhesion of phage 187 on living *Staphylococcus aureus* cells. We found that addition of free *N*-acetyl-*D*-glucosamine was able to decrease phage adhesion, suggesting that this monosaccharide plays major role in phage 187 infection of *S. aureus*. Moreover, phage 187 adhesion on monosaccharide-coated model surfaces combined with plaque forming unit counts suggested that a direct link can be established between the propensity to bind to a saccharide and the capability of the latter to inhibit phage infection. On a nanoscale level, single-particle force spectroscopy was successfully used to identify a major receptor required for phage 187 infection of *S. aureus* but also evidenced that this receptor was responsible for phage adhesion on host-cells. Our work demonstrates that single-particle force spectroscopy is a powerful platform to screen and predict the molecular target of phages on their host surfaces.

KEYWORDS

Atomic force microscopy, Single-particle force spectroscopy, Phage 187, *S. aureus*, Phage-bacteria interactions

1. INTRODUCTION

Phages are viruses that infect specific bacteria and that can undergo two different life cycles: lysogenic and lytic [1-3]. Lysogenic phages are known to be one of the causes for the increase of multi drug resistance as they promote horizontal gene transfer (HGT) among bacteria [4]. Lytic phages, on the other hand, are suggested to be one of the solutions for the raise of antibiotic-resistant pathogens with phage therapy as they can infect and rapidly kill these pathogens [5-8]. Phages are commercially available as biocontrol agents to help prevent colonization by pathogenic bacteria in agriculture, livestock and food production [9-11], and they present potential applications in wastewater treatment as a method of controlling pathogens in sewage water [12, 13]. After being eclipsed by the use of antibiotics for decades, phages have been regaining attention in the last years due to their implications in the raise of antibiotic-resistant infections and because of their vast potential of applications as antimicrobial agents.

All viruses including phages start their infection cycle by non-specific and specific interactions at the surface of their host cells [3, 14]. The recognition of the specific receptor is a key point in the host spectrum of a phage. While very little is known about non-specific interactions, some specific phage receptors are known, but again knowledge remains limited. Recognition is achieved by phage receptor binding proteins (RBPs) and is dependent on location of their target receptors on the bacteria wall surface as well as chemical and structural peculiarities [3, 14-17]. RBPs have strong affinities for specific receptors and allow phages to anchor on their host. Phages have single- or double-stranded DNA or RNA genome surrounded by a capsid. For the vast majority of phages (around 96%), the capsid (or the head) is connected to a protein tail that has RBPs at its other end [18]. Once anchored onto the cell surface, phages can inject their genetic material inside the host cell by using peptidoglycan hydrolases to degrade cell wall locally without lysing the bacteria. Host cells provide the molecular building blocks and enzymes required to replicate phages and produce progeny [1-3].

Understanding and characterizing phage-bacteria interactions is critical as they dictate infection [15]. In parallel of genomic and microbiology characterization, physico-chemical characterization of phages gave decisive insights notably through atomic force microscopy (AFM) which contributed intensively in imaging and characterizing the infection process of phages [19-21]. AFM-based force spectroscopy was revealed to be a powerful tool to characterize bacteria interactions with the use of single-molecule force spectroscopy (SMFS) and single-cell force spectroscopy (SCFS) [22-26]. For instance, AFM has already been used to decipher functions of viral attachment proteins in the initiation of infection with reovirus-decorated tips by SMFS on living cells [27]. AFM enables *in situ* characterization of living bacterial cells interactions with phages. However, most studies on living cells focus on the effects of phage infections on bacteria but very few studies focused on phage interactions themselves with single living host-cells to investigate adhesion [21, 28, 29]. In this work, we focus on specific recognition of living *Staphylococcus aureus* cells by phage 187 which belongs to the *Siphoviridae* family [30]. *S. aureus*, a Gram-positive bacterium, is a human pathogen of major concerns that can colonize a large variety of tissues in the body [31]. It commonly causes superficial and invasive infections leading to severe morbidity and mortality [32]. Treatments of *S. aureus* infections rely on long-term antibiotics which led to the raise of resistant strains such as methicillin-resistant *S. aureus* (MRSA) [33]. In Gram-positive bacteria, lipoteichoic acid (LTA) along with wall teichoic acid (WTA) are two of the major components of the cell envelop and are critical for growth, survival and pathogenicity [34, 35]. LTA and WTA form a polyanionic barrier that is required to maintain metal cation homeostasis and assist in transfers of ions, nutrients and proteins [36-38]. Peptidoglicans (PG) in the cell wall form a network on which polymers like WTA, polysaccharides and proteins are covalently linked. *S. aureus* WTA is generally made of repeating units composed of 1,5-D-ribitol-phosphate (RboP) tailored with *D*-alanine esters and mono- or oligosaccharides, commonly *N*-acetyl-*D*-glucosamine (GlcNAc) or *N*-acetyl-*D*-galactosamine (GalNAc) in certain cases [35, 39-41].

In the present study, AFM-based single particle force spectroscopy (SPFS) was used to map and probe interactions between single living *S. aureus* cells and phage 187 (Figure 1a). Effects of addition of free monosaccharides on phage infectivity were investigated as well as phage interactions with different monosaccharide-coated model surfaces. Because of *S. aureus* wall composition, GlcNAc and GalNAc were selected as the investigated monosaccharides along with their non-amino homologues: glucose (Glc) and galactose (Gal). This study provided valuable insights into the correlation between the specific ability of phage 187 to adhere on monosaccharide-coated surfaces and the capability of the monosaccharides to inhibit phage infection. On a nanoscale level, SPFS was used to identify a major receptor responsible for phage adhesion on host-cells and thus, a major receptor for phage infection initiation. Our findings helped building a predictive model designed to select best suitable saccharides to reduce phage infectivity by screening saccharide-coated model surfaces with phage-decorated AFM probes. Models developed with SPFS can also be used to predict molecular targets of phages on their host surfaces. This study expands the repertoire of AFM-based force spectroscopy and provides insights into correlation between phage adhesion and infectivity.

2. MATERIALS AND METHODS

2.1. Bacteria strains and phage 187.

Staphylococcus aureus phage 187 (HER 239) and *Staphylococcus aureus* strain 187 (HER 1239) were provided by Félix d'Hérelle Reference Center for Bacterial Viruses from the Université Laval (Québec, Canada). Phages were purified as previously described [42]. Briefly, after replication, phage 187 suspensions were centrifugated at 4,000 *g* for 20 min at 4°C and the supernatant was filtered using a 0.45 µm membrane (Millex®-GP, Millipore). Then 30 mL of this suspension was concentrated in 10 mL by Amicon Ultra-15 (PLHK, membrane Ultracel-PL, 100 kDa) by centrifugation at 1,000 *g* for 3 min. The phage suspension (2.5 mL) was purified by cesium chloride gradient after addition of 3.88 g CsCl (final volume: 6 mL) and centrifugation at 113,000 *g* for 18h at 15°C. About 1.5 mL of phage suspension was extracted from

central strip and then purified by dialysis (100 kDa molecular weight cutoff, Spectrum) against phosphate buffered saline (0.1X) for 14 h. The concentration of phages 187 obtained following the above protocol reached 10^9 PFU/mL. *S. aureus* was routinely grown at 37°C in tryptic soy broth (TSB) media. For phage infection, 10^2 PFU/mL of phage 187 was incubated with or without free monosaccharides (final concentration 10 mM) in Tris Buffered Saline supplemented with 1 mM $CaCl_2$ and $MgSO_4$ during 2h at room temperature under gentle agitation. *S. aureus* was cultivated in complemented tryptic soy broth to log-phase (OD_{600}, approximately 0.2) and infected with equal volume of phage 187. Phages were allowed to absorb for 5 min on *S. aureus* before plating on complemented tryptic soy agar (TSA) for titration.

2.2. Surface and AFM tip functionalization with phages.

Phages were attached covalently on self-assembled monolayers (SAM) of carboxyl-terminated alkanethiols. Briefly, gold substrates and gold coated NPG-D (Bruker) AFM tips were immersed overnight in a solution of 0.1 mM 16-mercaptododecahexanoic acid and 0.9 mM 11-mercapto-1-undecanol to form the SAM. Then, they were washed with ethanol, dried under N_2 flow and carboxylic groups were activated by immersion 30 min in a solution of N-hydroxysuccinimide (NHS, 20 mg/mL) and 1-ethyl-3-(3-dimethylaminopropyl)-carbodiimide (EDC, 50 mg/mL). After rinsing with ultrapure water, 2 x 10^8 PFU of purified phages were added for 1 hour. NHS/EDC coupling formed strong covalent amide bonds between the carboxylic group of the 16-mercaptododecahexanoic acid thiol present on the functionalized gold-coated tips and the amine groups from the phage surface. Finally, surfaces and tips were rinsed in TBS buffer containing 1 mM $CaCl_2$ and $MgSO_4$ (TBS^+) and stored for max. 48 h in the same buffer until their use. For AFM images in air, surfaces were gently rinsed in 3 baths of ultrapure water and let to dry overnight at 30°C before imaging.

2.3. AFM imaging and force spectroscopy.

All experiments were achieved at room temperature using a Bioscope Resolve AFM (Bruker corporation, Santa Barbara, CA) and cantilevers spring constants were determined by the thermal noise method [43].

Phage immobilized on substrates were imaged in peak-force tapping mode using HIRS-F-B tips in air or in TBS^+. For force measurements on cells, stationary phase cultures of *S. aureus* were centrifuged, washed twice in TBS^+ and filtered into porous polycarbonate membranes (Millipore). After filtration and rinsing, a 1 x 1 cm^2 piece of membrane was cut and attached with double sided adhesive tape at the bottom of a Petri dish and immersed in TBS^+. First, bare SNL-D tips were used to localize and image individual cells. Then, the tip was replaced by phage decorated tip and adhesion maps of 32 x 32 FD curves on areas of 500 x 500 nm^2 were recorded on the cell surface with 250 pN applied force, 1 µm/s constant approach and retraction speeds and 250 ms contact time. For inhibition tests, 10 mM of free monosaccharides were added to the Petri dish and adhesion maps were subsequently recorded on the same cells. For force spectroscopy on monosaccharide-coated model surfaces, silicon substrates were immersed overnight in a mixture of 0.9 mM tetraethoxysilane (TEOS, $Si(OCH_2CH_3)_4$), and 0.1 mM isocyanatopropyltriethoxysilane (ICPTES, $(C_2H_5O)_3Si(CH_2)_3NCO$) for silanization and functionalization with isocyanate moieties. Then, they were washed with ethanol, dried under N_2 flow and immersed in 10 mM GlcNAc, GalNAc, Glc and Gal for 24 hours. Monosaccharide coated substrates were then rinsed with TBS^+, imaged in contact mode with bare SNL-D tips and probed with phage decorated NPG-D tips by recording adhesion maps of 5 x 5 μm^2.

3. RESULTS AND DISCUSSION

3.1. Phage 187 infects S. aureus and can be grafted on gold-coated AFM cantilevers.

The first step of this study was to evaluate the infectivity of phage 187 on *S. aureus* by phage plaque assay. Briefly, lysis plaques are clear zones that appear in a homogenous bacteria culture on agar medium due to lysis by phages. Presence of lysis plaques shows the ability of the phage to infect and lyse the bacteria. Lysis plaques are the result of cycles of infection due to one phage (or one aggregate of phages) and occurring cell by cell in all directions from the original infection center thus producing circular areas of lysis called plaque forming unit (PFU) [44]. They represent a simple, cost-efficient and fast technique to

evidence and quantify phage infection [45]. When *S. aureus* cells were in contact with purified phages 187, lysis plaques of ~1 mm in diameter were observed (Figure 1b).

To probe the interactions between phage 187 and *S. aureus*, we hypothesized that phages can be covalently grafted on gold coated AFM tips using N-hydroxysuccinimide/N-(3-dimethyl-aminopropyl)-N'-ethylcarbodiimide hydrochloride (NHS/EDC) coupling. To confirm this hypothesis, we first functionalized and imaged flat gold substrate. Figure 2 shows topography images of phages covalently attached on gold-coated substrates. Phage 187 is known to have polyhedral shaped heads connected to a tubbed-like tail [46]. In air, the typical shape of S*iphoviridae* was confirmed with the presence of polyhedral heads linked to tails (Figure 2a). Imaging single phage at high resolution revealed a full length of ~200 nm with a head of ~65 nm from the apex to the head-tail joint and a tail length of ~140 nm (Figure 2b). Head height was estimated at ~10 nm and the tail revealed a tubbed-like shape of around 6 nm in height. These morphological features are in good accordance with previous observations of phage 187 achieved by electron microscopy [46]. At the distal end of the tail, an increase of height was observed. We associated it to the baseplate of the phage to which RBPs are attached as already suggested with other phages observed by AFM in the literature [47]. In liquid, the head height was ~25 nm (data not shown). We attributed this height difference to particle collapsing during air drying which is a common phenomenon in AFM phage observations [47]. Remarkably, whereas phage heads were successfully imaged in liquid, tails were not detected or appeared as poorly defined streaks (Figure 2c) probably because they were too flexible or too mobile and were pushed by the scanning tip. As phages were successfully observed in liquid and air, we concluded that phage 187 can be successfully attached to gold substrates. Phages grafted on gold-coated substrate using NHS/EDC coupling led to strong covalent amide bonds that resist forces superior to 2 nN [48, 49]. Therefore, as long as the forces measured by SMFS do not exceed the nanonewton, the amide bond between the phages and the gold-coated AFM tips was considered covalent and irreversible. Thus, we decided to use this approach to functionalize gold-coated AFM tips with phages

176 in order to measure their interaction with living *S. aureus* cell surfaces by mean of AFM-based SPFS (Figure
177 2d).

178 **3.2. Phage 187 recognizes *S. aureus* cell wall with high adhesion frequency.**

179 We probed single living *S. aureus cells* with phage-decorated AFM tips. Figure 3 and S1 show adhesion
180 maps, adhesion force and rupture length histograms as well as representative force-distance (FD) curves
181 obtained by SPFS on live bacteria. For all the cells, adhesion maps did not show cluster patterns, *i.e.*
182 adhesive pixels were randomly spread on the maps (Figure 3a and S1a). This suggested that phage
183 receptors were homogeneously distributed on the host cell surface. Most of the FD curves (51% to 91%
184 depending on the cell) showed adhesive peaks except for cell#S3 (Figure S1b-c) that showed an adhesion
185 frequency of only 17%. Variations in adhesion frequencies between cells were suggested to be caused by
186 slight heterogeneity in cell wall microarchitecture, and composition and/or the angle and position of
187 phage-decorated AFM cantilevers during measurements. Forces mainly ranged from 50 pN to 600 pN
188 (Figure 3b and S1b). This confirmed that phage-bacteria interactions forces were inferior than typical
189 covalent bond forces that exist between the phages and the AFM tips [48]. Thus, we considered that during
190 the repeating approaches and retractions of the AFM tips throughout measurements, weak bonds
191 between phages and cells ruptured before covalent bonds between the phages and the tips. This was
192 further confirmed by the consistent adhesion signatures obtained throughout all the measurements in
193 Figure 3 and S1 and also confirmed with the homogeneousness of the adhesion maps obtained. The
194 majority of rupture lengths ranged between 10 nm and 300 nm (Figure 3c and S1c). Representative FD
195 curves are presented in Figure 3c and S1c as examples. They show the retraction of the AFM tip decorated
196 with the phages. Some curves did not present any adhesion peaks and were considered as “non-adhesive
197 events”. By contrast, adhesive FD curves presented a single or multiple adhesion peaks that we attributed
198 to the interactions between the phage RBPs and the receptors on the cell wall.

3.3. SPFS reveals major cell wall receptors for phage adhesion.

Phage 187 showed homogenous recognition of *S. aureus* cell wall suggesting phage receptors are distributed evenly on the surface of cells. *S. aureus* WTA, which is one of the most abundant components in cell wall, generally presents repeating units composed of RboP with mono- or oligosaccharides residues like GlcNAc or GalNAc [35, 39-41]. We used SPFS to decipher phage interactions with GlcNAc and GalNAc in order to conclude if these monosaccharides lead to specific adhesion of phage 187. Specific adhesion would suggest a probable implication of these molecules in phage recognition process. Interactions with non-amino equivalents, Glc and Gal, were also deciphered. Effect of different monosaccharides on phage infectivity was first investigated at the population scale by incubating phage 187 with free monosaccharides and then quantifying infectivity by PFU counting (Figure 4). When 1×10^2 PFU of phage 187 was put in contact with free Glc, Gal, and GalNAc for 2h prior to infection, total phage-infected *S. aureus* cells decreased respectively of 22%, 12% and 37% compared to the absence of free monosaccharide. Remarkably, total inhibition was observed with free GlcNAc as no lysis plaques were observed suggesting that no infection occurred or infection was below the detection limit (Figure 4). This suggests that phage 187 RBPs were already saturated with free GlcNAc residues and thus were unable to adsorb and anchor to *S. aureus* cells. Therefore, infection process could not be initiated resulting in a total inhibition of infectivity.

To determine the effect of monosaccharides on phage adhesion at the single particle level, living cells were probed with AFM tips decorated with phage 187 in absence or presence of free monosaccharides. As previously discussed, slight quantitative heterogeneity in adhesion frequencies appeared that may be caused by heterogeneities in the cell population. To alleviate this possible undesired parameter and in order to compare the effect of monosaccharides on phage adhesion, the same cell was probed for each measurement before and after monosaccharide addition (Figure 5). *S. aureus* cells were immobilized in porous membranes (Figure 5a). Figure 5b shows the adhesion force histograms obtained without

monosaccharide and Figure 5c displays the adhesion force histograms for the same cells with different monosaccharides supplemented in the media. In absence of free monosaccharides, frequencies of adhesive events ranged from 69% to 82% (Figure 5b). When free monosaccharides were added to the media, a decrease in adhesion was observed and frequencies of adhesive events ranged from 25% to 61% (Figure 5c). For all conditions, the number of phage adhesive events on cells decreased but the intensity of interactions, *i.e.* the range of adhesion forces, stayed the same (Figure 5b *vs* 5c). Adhesion frequency decreased from 76% to 42% (*i.e.* a delta of 34%) when free Glc was added in media (Figure 5). With the presence of free GlcNAc, a decrease of adhesion was also observed from 82% to 25% (*i.e.* a delta of 57%). This shows that phage 187 adhesion on *S. aureus* was less prone to happen in presence of free GlcNAc than in presence of free Glc, suggesting that the acetyl amino group of GlcNAc plays a role in phage adhesion and recognition. In presence of free GalNAc, a delta of 33% of adhesive events was observed (from 72% with no GalNAc to 39% with GalNAc). However, the addition of free Gal in the media showed almost no effect on phage adhesion with a variation of adhesion frequency from 69% without Gal to 61% with free Gal (*i.e.* a delta of 8%). Decrease in phage adhesion was more important with free GalNAc compared to free Gal suggesting once again that the acetyl amino group plays a role in phage adhesion and recognition. To confirm these observations, SPFS was repeated on multiple cells. Moreover, the concentration of monosaccharide used is not known to cause any damages to cell walls [50]. But to alleviate any possible contribution of the monosaccharides in the alteration of adhesion signatures and cell integrity, control cells were imaged before and after monosaccharide addition. Addition of monosaccharides did not alter the morphology of bacterial cell wall (Figure S3) thus we assumed that monosaccharides did not cause any damage to the cells that could have altered the adhesion signatures. Figure 6 regroups the results obtained with four cells per monosaccharide tested. GlcNAc induced once more the most important adhesion decrease with a mean delta of 53% ± 4% whereas adhesion decreased by only 15% ± 6% with free Glc. GalNAc and Gal led to a decrease of 24%±6% and 9%±2%, respectively.

This confirmed that phage 187 had lessened abilities to adhere on cell wall surface when free GlcNAc, GalNAc or Glc are added in the media and that the acetyl amino groups of GlcNAc and GalNAc play a role on phage adhesion.

3.4. Monosaccharide-coated model surfaces coupled with SPFS can help predict monosaccharide effects of phage inhibition.

In order to confirm the specific interaction of phage 187 with different monosaccharides and exclude possible effects of other cell wall components, model surfaces coated with monosaccharides were developed. Model surfaces coated with GlcNAc, GalNAc, Glc and Gal were probed with phage-decorated tip to screen the affinity of phage 187 for each monosaccharide independently (Figure 7a). Topography images of the coated surfaces revealed smooth and homogeneous deposition for all samples with a thickness of ~1.3 nm (Figure 7b). Phage 187 presented high adhesion frequency towards GlcNAc model surfaces (Figure 7c). Adhesion events represented around 93% of the total FD curves for the surface coated with GlcNAc whereas for GalNAc, Gal and Glc, only 32%, 16% and 14% of the FD curves corresponded to adhesive events, respectively. Monosaccharide containing acetyl amino groups led to higher adhesion frequencies than homologous molecules lacking acetyl amino groups. Phage 187 had strongest affinities with these monosaccharides (GlcNAc and GalNAc) which is consistent to the inhibition results of phage 187 infectivity in presence of the free monosaccharides. Figure S2 shows three independent SPFS acquisitions on GlcNAc-coated model surfaces. Similarly to acquisitions on cells, adhesion maps on model surfaces revealed an homogeneous distribution of adhesion events (Figure S2a). Adhesion forces ranged from 150 pN to around 700 pN (Figure S2b) which was higher than adhesion forces on cell surfaces. This difference could be explained by a higher density of saccharides on the model surfaces than on the cell wall surface and/or the absence of interferences with other molecules present on the bacteria surface. Rupture lengths however were lower on model surfaces than when SPFS was performed on cells and ranged from 50 to 100 nm (Figure S2c). Molecules grafted on model surfaces were monosaccharides

whereas saccharides in *S. aureus* cell wall are mostly in the form of residues in long glycopolymer chains like WTA [35, 39-41]. The difference in the length, and thus in elasticity, between these molecules could explain the lower rupture lengths and the different FD curve signatures observed when monosaccharide-coated model surfaces were scanned by SPFS.

Phage-infected *S. aureus* proportion in presence of a monosaccharide was correlated to the adhesion frequency of phage 187 on a model surface coated with the same monosaccharide (Figure 8). In other terms the higher adhesion forces between a monosaccharide (GlcNAc, GalNAc, Glc and Gal) and phage 187 are, the better this saccharide will be in inhibiting phage infection. This relationship between adhesion to model surfaces and inhibition of infection can help predict the infectivity of phage 187 on *S. aureus* in presence of a saccharide by screening the adhesion of the phages on a saccharide-coated model surfaces. It would be relevant to test with other saccharides and phages to build a predictive model by extrapolation where screening adhesion forces of a phage with saccharide coated surfaces can help predict the inhibition potential of this saccharide with a specific phage.

4. **CONCLUSIONS**

With the raise of antibiotic-resistant infections, thorough understanding of phage-host adhesion becomes crucial. This work demonstrates the potential of single-particle force spectroscopy, a homologous technique to single-molecule force spectroscopy and single-cell force spectroscopy, to reveal major cell wall receptors for phages and to help identify best suitable phage infection inhibitors. Phage-decorated atomic force microscopy tips were successfully used to screen phage adhesion on single living cells and on model surfaces coated with molecules of interest. Single-particle force spectroscopy evidenced affinities of phage 187 for monosaccharides presenting acetyl amino groups. It also evidenced that these monosaccharides were able to reduce phage adhesion on *S. aureus* cells after a contact of 2h. Single-particle force spectroscopy combined with plaque forming unit counts showed a direct correlation

between phage 187 infectivity in presence of *N*-acetyl-*D*-glucosamine, *N*-acetyl-*D*-galactosamine, glucose and galactose and phage adhesion forces on coated surfaces with these saccharides. This suggested that the higher adhesion forces between a saccharide and phage 187 are, the better this saccharide will be in inhibiting phage infection of *S. aureus*. Single-particle force spectroscopy can help identifying the relationship between the propensity of an inhibitor to bind to phages and the efficacy of inhibition in order to develop models that can predict efficacy of inhibitor only by characterizing phage-inhibitor interactions, for faster inhibitor characterization, and that helps choosing the best suitable inhibitor. This study expands the repertoire of atomic force microscopy-based force spectroscopy and provides insights on correlation between phage adhesion and infectivity.

ACKNOWLEDGEMENTS

We thank the Félix d'Hérelle Reference Center for Bacterial Viruses from the Université Laval (Canada) for providing the phage and the host strain. This work was supported by the Agence Nationale de la Recherche (ANR-20-CE06-0001), the Zone Atelier Moselle (ZAM) and the Lorraine Université d'Excellence (ANR-15-IDEX-04-LUE). We would also like to thank Chloé Retourney and Julie Challant for their help.

The authors declare no competing interests.

AUTHOR CONTRIBUTIONS

B.A., M.G., C.G., N.V., I.B. and S.E.K.C designed research; B.A., M.G., N.V. and S.E.K.C performed research; B.A., M.G., C.G., N.V., I.B. and S.E.K.C analyzed data; B.A., M.G., C.G., I.B. and S.E.K.C wrote the original draft.

ELECTRONIC SUPPLEMENTARY MATERIAL (ESM)

Supplementary material (Figure S1 and S2 showing additional adhesion maps recorded on *S. aureus* cells and on GlcNAc-coated model surfaces with AFM tips decorated with phage 187 and Figure S3 showing the impact of GlcNAc on cell wall) is available in the online version of this article.

REFERENCES

[1] Clokie, M. R.; Millard, A. D.; Letarov, A. V.; Heaphy, S. Phages in nature. *Bacteriophage* **2011**, *1*, 31-45.

[2] Doss, J.; Culbertson, K.; Hahn, D.; Camacho, J.; Barekzi, N. A review of phage therapy against bacterial pathogens of aquatic and terrestrial organisms. *Viruses* **2017**, *9*, 50.

[3] Dowah, A. S.; Clokie, M. R. Review of the nature, diversity and structure of bacteriophage receptor binding proteins that target Gram-positive bacteria. *Biophys. Rev.* **2018**, *10*, 535-542.

[4] Winstel, V.; Liang, C.; Sanchez-Carballo, P.;Steglich, M.; Munar, M.; Bröker, B. M.; Penadés, J. R.;Nübel, U.; Holst, O.; Dandekar, T. Wall teichoic acid structure governs horizontal gene transfer between major bacterial pathogens. *Nat. Commun.* **2013**, *4*, 1-9.

[5] Chan, B. K.; Abedon, S. T.; Loc-Carrillo, C. Phage cocktails and the future of phage therapy. *Future Microbiol.* **2013**, *8*, 769-783.

[6] Moelling, K.; Broecker, F.; Willy, C. A wake-up call: we need phage therapy now. *Viruses* **2018**, *10*, 688.

[7] Azam, A. H.; Tanji, Y. Peculiarities of Staphylococcus aureus phages and their possible application in phage therapy. *Appl. Microbiol. Biotechnol.* **2019**, *103*, 4279-4289.

[8] Sulakvelidze, A.; Alavidze, Z.; Morris Jr, J. G. Bacteriophage therapy. *Antimicrob. Agents Chemother.* **2001**, *45*, 649-659.

[9] Jamal, M.; Bukhari, S. M.; Andleeb, S.; Ali, M.; Raza, S.; Nawaz, M. A.; Hussain, T.; Rahman, S. U.; Shah, S. S. Bacteriophages: an overview of the control strategies against multiple bacterial infections in different fields. *J. Basic Microbiol.* **2019**, *59*, 123-133.

[10] Sarhan, W. A.; Azzazy, H. M. Phage approved in food, why not as a therapeutic? *Expert Rev Anti Infect Ther* **2015**, *13*, 91-101.

[11] Żbikowska, K.; Michalczuk, M.; Dolka, B. The use of bacteriophages in the poultry industry. *Animals* **2020**, *10*, 872.

[12] Withey, S.; Cartmell, E.; Avery, L.; Stephenson, T. Bacteriophages—potential for application in wastewater treatment processes. *Sci. Total Environ.* **2005**, *339*, 1-18.

[13] Periasamy, D.; Sundaram, A. A novel approach for pathogen reduction in wastewater treatment. *J. Environ. Health Sci. Eng.* **2013**, *11*, 1-9.

[14] Bertozzi Silva, J.; Storms, Z.; Sauvageau, D. Host receptors for bacteriophage adsorption. *FEMS Microbiol. Lett.* **2016**, *363*, fnw002.

[15] Stone, E.; Campbell, K.; Grant, I.; McAuliffe, O. Understanding and exploiting phage–host interactions. *Viruses* **2019**, *11*, 567.

[16] Rakhuba, D.; Kolomiets, E.; Dey, E. S.; Novik, G. Bacteriophage receptors, mechanisms of phage adsorption and penetration into host cell. *Polish J. Microbiol.* **2010**, *59*, 145.

[17] Bielmann, R.; Habann, M.; Eugster, M. R.; Lurz, R.; Calendar, R.; Klumpp, J.; Loessner, M. J. Receptor binding proteins of Listeria monocytogenes bacteriophages A118 and P35 recognize serovar-specific teichoic acids. *Virology* **2015**, *477*, 110-118.

[18] Ackermann, H.-W. Bacteriophage observations and evolution. *Res. Microbiol.* **2003**, *154*, 245-251.

[19] Dubrovin, E. V.; Voloshin, A. G.; Kraevsky, S. V.; Ignatyuk, T. E.; Abramchuk, S. S.; Yaminsky, I. V.; Ignatov, S. G. Atomic force microscopy investigation of phage infection of bacteria. *Langmuir* **2008**, *24*, 13068-13074.

[20] Zago, M.; Scaltriti, E.; Fornasari, M. E.; Rivetti, C.; Grolli, S.; Giraffa, G.; Ramoni, R.; Carminati, D. Epifluorescence and atomic force microscopy: two innovative applications for studying phage–host interactions in Lactobacillus helveticus. *J. Microbiol. Methods* **2012**, *88*, 41-46.

[21] Alsteens, D.; Trabelsi, H.; Soumillion, P.; Dufrêne, Y. F. Multiparametric atomic force microscopy imaging of single bacteriophages extruding from living bacteria. *Nat. Commun.* **2013**, *4*, 1-7.
[22] Müller, D. J.; Dufrene, Y. F. Atomic force microscopy as a multifunctional molecular toolbox in nanobiotechnology. *Nanosci. Technol.* **2010**, 269-277.
[23] Helenius, J.; Heisenberg, C.-P.; Gaub, H. E.; Muller, D. J. Single-cell force spectroscopy. *J. Cell Sci.* **2008**, *121*, 1785-1791.
[24] El-Kirat-Chatel, S.; Beaussart, A. Probing bacterial adhesion at the single-molecule and single-cell levels by AFM-based force spectroscopy. In *Nanoscale Imaging*. Springer, 2018; pp 403-414.
[25] Beaussart, A.;Feuillie, C.; El-Kirat-Chatel, S. The microbial adhesive arsenal deciphered by atomic force microscopy. *Nanoscale* **2020**, *12*, 23885-23896.
[26] Beaussart, A.; El-Kirat-Chatel, S. Microbial adhesion and ultrastructure from the single-molecule to the single-cell levels by Atomic Force Microscopy. *Cell Surf* **2019**, *5*, 100031.
[27] Koehler, M.; Aravamudhan, P.; Guzman-Cardozo, C.; Dumitru, A. C.; Yang, J.; Gargiulo, S.;Soumillion, P.; Dermody, T. S.; Alsteens, D. Glycan-mediated enhancement of reovirus receptor binding. *Nat. Commun.* **2019**, *10*, 1-14.
[28] Liu, S.; Wang, Y. Application of AFM in microbiology: a review. *Scanning* **2010**, *32*, 61-73.
[29] Dubrovin, E. V.; Popova, A. V.; Kraevskiy, S. V.; Ignatov, S. G.; Ignatyuk, T. E.; Yaminsky, I. V.; Volozhantsev, N. V. Atomic Force Microscopy Analysis of the Acinetobacter baumannii Bacteriophage AP22 Lytic Cycle. *PLoS ONE* **2012**, *7*, e47348.
[30] Deghorain, M.; Van Melderen, L. The Staphylococci phages family: an overview. *Viruses* **2012**, *4*, 3316-3335.
[31] Wertheim, H. F.; Melles, D. C.; Vos, M. C.; Van Leeuwen, W.; Van Belkum, A.; Verbrugh, H. A.; Nouwen, J. L. The role of nasal carriage in Staphylococcus aureus infections. *Lancet Infect. Dis.* **2005**, *5*, 751-762.
[32] Ford, C. A.; Hurford, I. M.; Cassat, J. E. Antivirulence strategies for the treatment of Staphylococcus aureus infections: a mini review. *Front. Microbiol.* **2021**, *11*, 3568.
[33] Lindsay, J. A.; Holden, M. T. Understanding the rise of the superbug: investigation of the evolution and genomic variation of Staphylococcus aureus. *Functional & integrative genomics* **2006**, *6*, 186-201.
[34] Seo, H. S.; Cartee, R. T.; Pritchard, D. G.; Nahm, M. H. A new model of pneumococcal lipoteichoic acid structure resolves biochemical, biosynthetic, and serologic inconsistencies of the current model. *J. Bacteriol.* **2008**, *190*, 2379-2387.
[35] Brown, S.; Santa Maria Jr, J. P.; Walker, S. Wall teichoic acids of gram-positive bacteria. *Annu. Rev. Microbiol.* **2013**, *67*, 313-336.
[36] Hughes, A.; Hancock, I.; Baddiley, J. The function of teichoic acids in cation control in bacterial membranes. *Biochem. J.* **1973**, *132*, 83-93.
[37] Lambert, P. A.; Hancock, I. C.; Baddiley, J. Occurrence and function of membrane teichoic acids. *Biochim. Biophys. Acta* **1977**, *472*, 1-12.
[38] van Wely, K. H.; Swaving, J.; Freudl, R.; Driessen, A. J. Translocation of proteins across the cell envelope of Gram-positive bacteria. *FEMS Microbiol. Rev.* **2001**, *25*, 437-454.
[39] Xia, G.; Maier, L.; Sanchez-Carballo, P.; Li, M.; Otto, M.; Holst, O.; Peschel, A. Glycosylation of wall teichoic acid in Staphylococcus aureus by TarM. *J. Biol. Chem.* **2010**, *285*, 13405-13415.
[40] Mnich, M. E.; Van Dalen, R.; Gerlach, D.; Hendriks, A.; Xia, G.; Peschel, A.; Van Strijp, J. A.; Van Sorge, N. M. The C-type lectin receptor MGL senses N-acetylgalactosamine on the unique Staphylococcus aureus ST395 wall teichoic acid. *Cell. Microbiol.* **2019**, *21*, e13072.
[41] Winstel, V.; Sanchez-Carballo, P.; Holst, O.; Xia, G.; Peschel, A. Biosynthesis of the unique wall teichoic acid of Staphylococcus aureus lineage ST395. *MBio* **2014**, *5*, e00869-00814.

[42] Bacharouche, J.; Erdemli, O.; Rivet, R.; Doucoure, B.; Caillet, C.; Mutschler, A.; Lavalle, P.; Duval, J. F. L.; Gantzer, C.; Francius, G. On the Infectivity of Bacteriophages in Polyelectrolyte Multilayer Films: Inhibition or Preservation of Their Bacteriolytic Activity? *ACS Appl Mater Interfaces* **2018**, *10*, 33545-33555.
[43] Hutter, J. L.; Bechhoefer, J. Calibration of atomic-force microscope tips. *Review of scientific instruments* **1993**, *64*, 1868-1873.
[44] You, L.; Yin, J. Amplification and spread of viruses in a growing plaque. *J. Theor. Biol.* **1999**, *200*, 365-373.
[45] Gallet, R.; Kannoly, S.; Wang, N. Effects of bacteriophage traits on plaque formation. *BMC Microbiol.* **2011**, *11*, 1-16.
[46] Bradley, D.; Kay, D. The fine structure of bacteriophages. *Microbiology* **1960**, *23*, 553-563.
[47] Kuznetsov, Y. G.; Chang, S.-C.; McPherson, A. Investigation of bacteriophage T4 by atomic force microscopy. *Bacteriophage* **2011**, *1*, 165-173.
[48] Grandbois, M.; Beyer, M.; Rief, M.; Clausen-Schaumann, H.; Gaub, H. E. How strong is a covalent bond? *Science* **1999**, *283*, 1727-1730.
[49] Herman, P.; El-Kirat-Chatel, S.; Beaussart, A.; Geoghegan, J. A.; Foster, T. J.; Dufrêne, Y. F. The binding force of the staphylococcal adhesin SdrG is remarkably strong. *Mol. Microbiol.* **2014**, *93*, 356-368.
[50] Komatsuzawa, H.; Fujiwara, T.; Nishi, H.; Yamada, S.; Ohara, M.; McCallum, N.; Berger-Bächi, B.; Sugai, M. The gate controlling cell wall synthesis in Staphylococcus aureus. *Mol. Microbiol.* **2004**, *53*, 1221-1231.

433 **FIGURES**

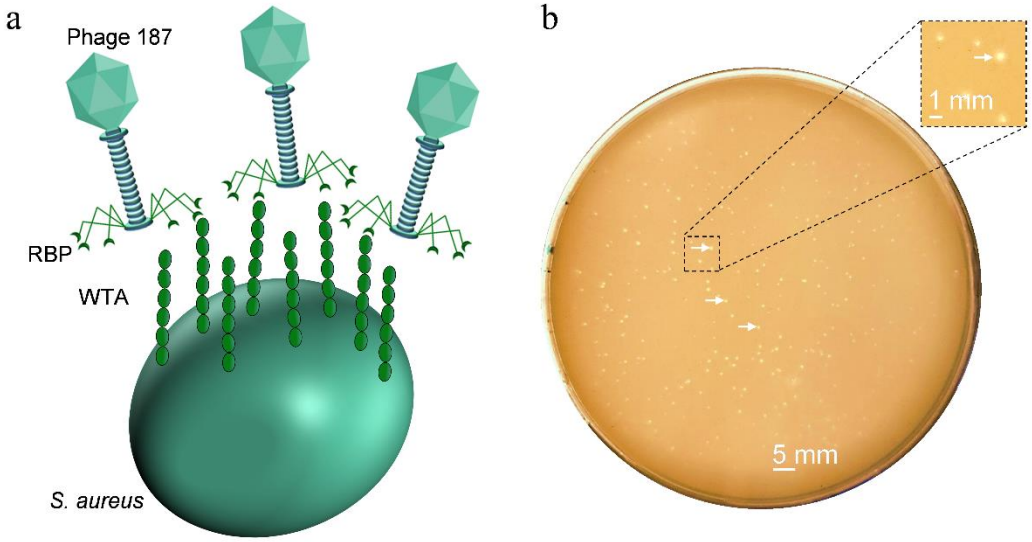

434

435 **Figure 1.** (a) Schematic of the interaction between the phage 187 and *S. aureus.* The phage receptor-
436 binding proteins (RBPs) recognize sub-units of the peptidoglycan-anchored wall teichoic acids (WTA) on *S.*
437 *aureus* surface. (b) PFU obtained after mixing 1 x 10^2 PFU of purified phage 187 with approximately 1 x 10^8
438 *S. aureus* cells in TSB medium supplemented with 1 mM $CaCl_2$ and 1 mM $MgSO_4$. A uniform bacterial mat
439 covered the TSA agar in the Petri dish. Bacterial infections lead to lysis plaques (clear dots) of ~1
440 mm diameter where bacteria were lysed and did not grow. For eyes guidance, three lysis plaques
441 are pointed with white arrows and a three-time zoom of a small area is added.

442

443
444

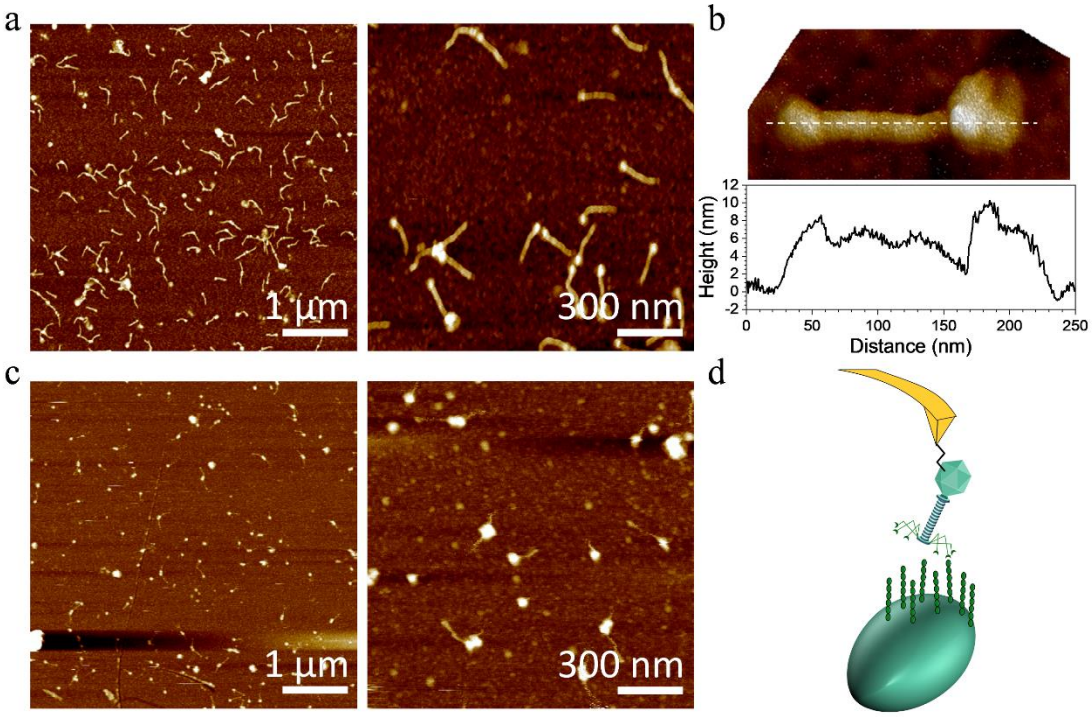

Figure 2. (a) AFM height images in air of purified phage 187 grafted by NHS/EDC coupling on gold-coated surfaces. (b) High resolution topography tridimensional image (500 x 500 nm) in air of a single phage 187 covalently immobilized on gold substrate and corresponding cross section taken along the dashed line on the height image. (c) AFM height images in buffer of purified phage 187 grafted by NHS/EDC coupling on gold-coated surfaces. (d) Principle of single particle force spectroscopy where AFM tips decorated with phage 187 are used to probe single *S. aureus* cells.

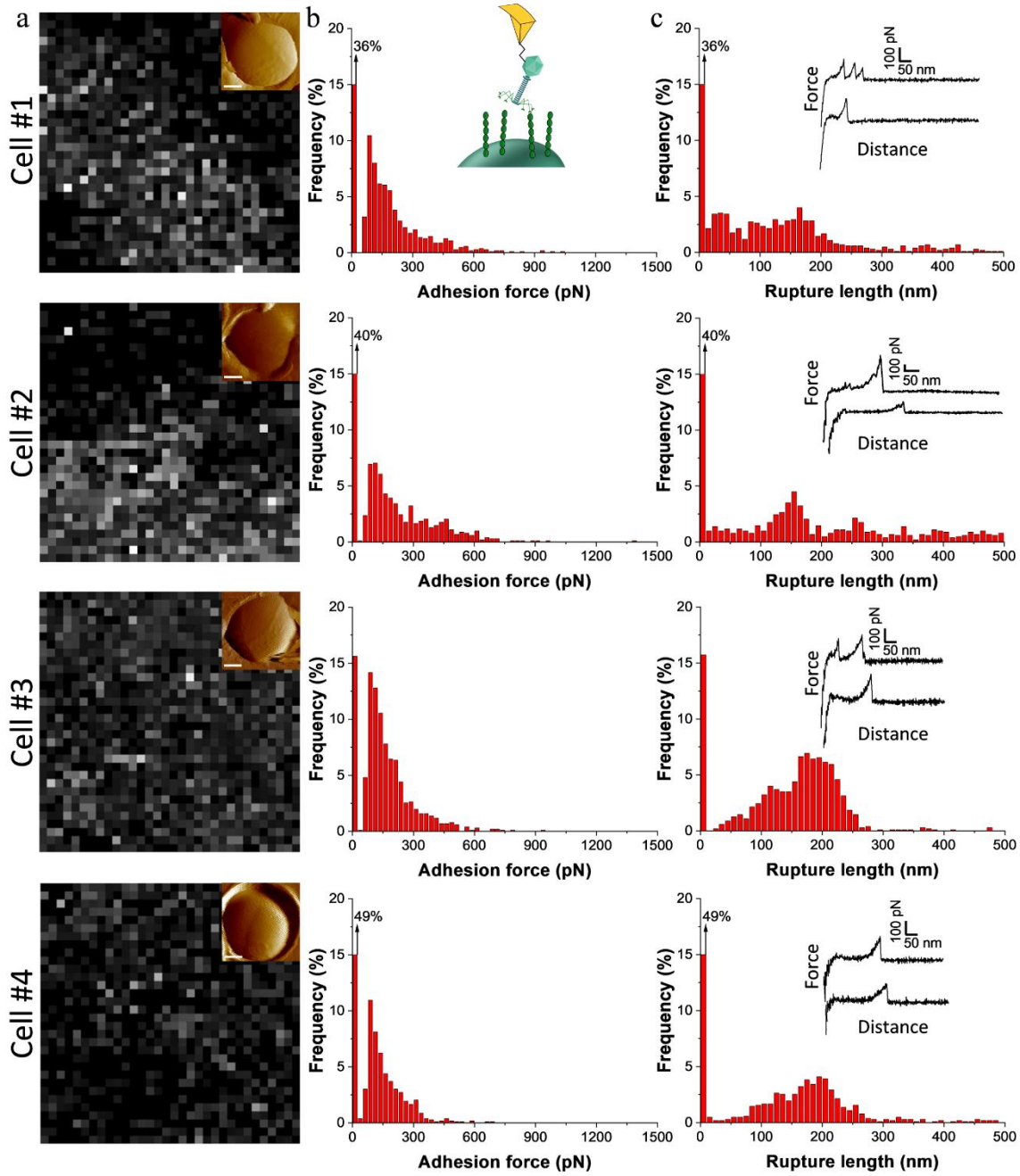

455

456 **Figure 3.** (a) Adhesion maps (500 x 500 nm²) recorded on *S. aureus* cells (insets, scale bar = 250 nm) with
457 AFM tips decorated with phage 187. White/grey pixels correspond to adhesive events and black pixels
458 correspond to non-adhesive events (scale 0-1000 pN). (b) Corresponding adhesion force and (c) rupture
459 length histograms together with representative force curves. Data were obtained from three independent
460 experiments using different tips and independent cultures.

461

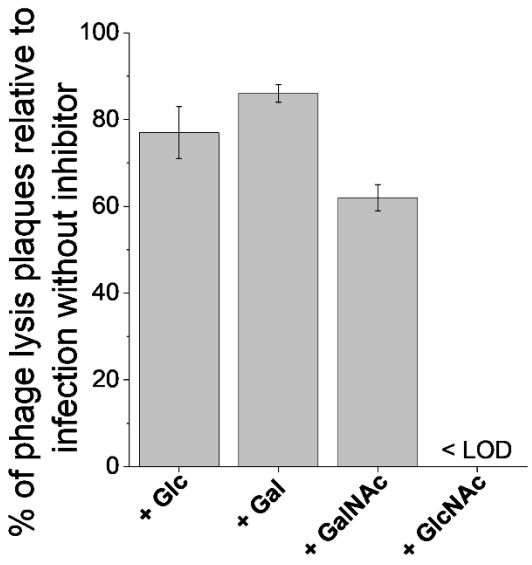

462

463 **Figure 4.** Infectivity of phage 187 towards *S. aureus* cells after 2 hours contact with free monosaccharides
464 (10 mM) determined by plaque forming unit (PFU) counting. *S. aureus* cells (1 x 10^8) were mixed with
465 phage 187 (1 x 10^2) and plated on growth media. The percentage of infection was determined by
466 comparison to the number of PFU in absence of free monosaccharides. (Glc: Glucose; Gal: Galactose;
467 GalNAc: N-acetyl-D-galactosamine; GlcNAc: N-acetyl-D-glucosamine; LOD: Limit of detection). Error bars
468 correspond to standard errors calculated from three independent experiments.

469

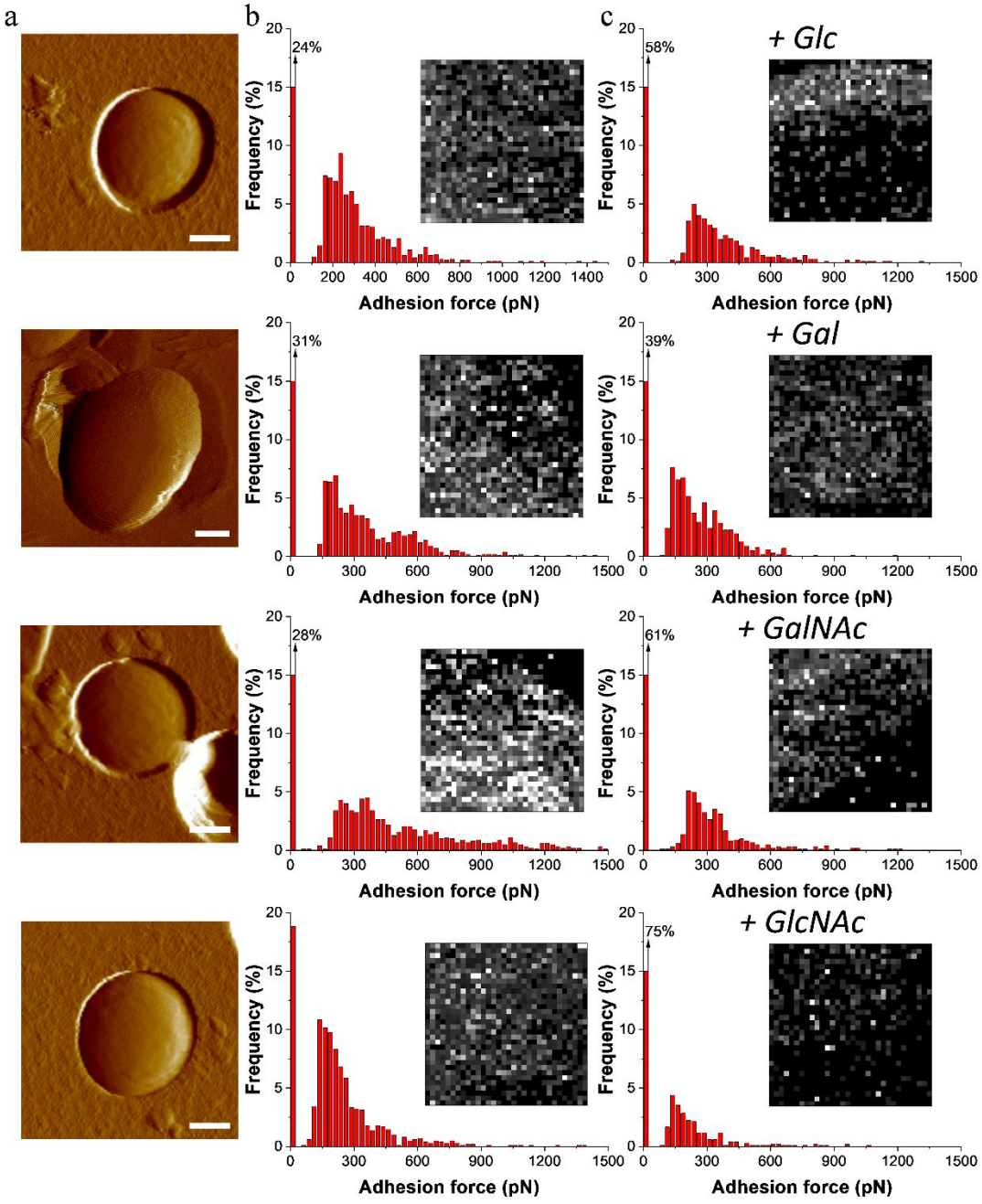

Figure 5. (a) Topography images of *S. aureus* cells trapped in porous membranes (scale bar = 250 nm) and probed with AFM tips decorated with phage 187. (b, c) Adhesion force histograms and adhesion force maps (500 x 500 nm², insets) obtained on cells (b) in the absence and (c) in the presence of free monosaccharides (10 mM). White/grey pixels correspond to adhesive events and black pixels correspond

475 to non-adhesive events (scale 0-1000 pN). The added free monosaccharides are indicated above the

476 adhesion force histograms in (c).

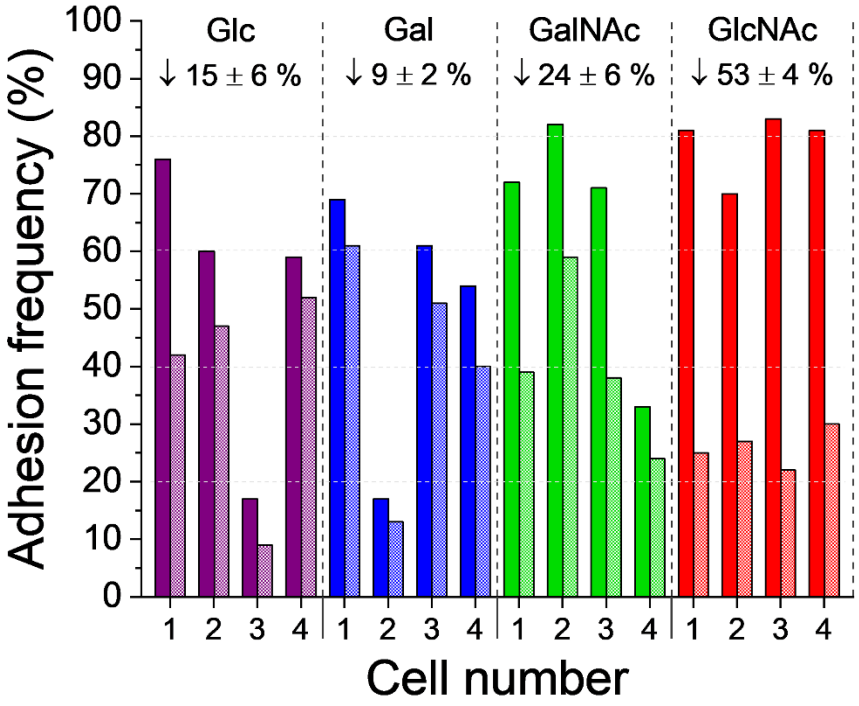

477

478 **Figure 6.** Adhesion frequency recorded between the surface of *S. aureus* cells and AFM tips decorated with
479 phage 187 with or without free monosaccharides (10 mM). For each monosaccharide, adhesion maps were
480 recorded on four cells (1-4) in absence (colored bars) or presence (patterned/light colored bars) of free
481 monosaccharides (10 mM) (Purple: Glc; Blue: Gal; Green: GalNAc; Red: GlcNAc). The average decrease is
482 indicated below each monosaccharide name (mean ± s.e.). The adhesion frequency was calculated from
483 the adhesive FD curves obtained among the 1024 FD curves recorded for each map. For each
484 monosaccharide, data were obtained from three independent experiments using different tips and
485 independent cultures.

486

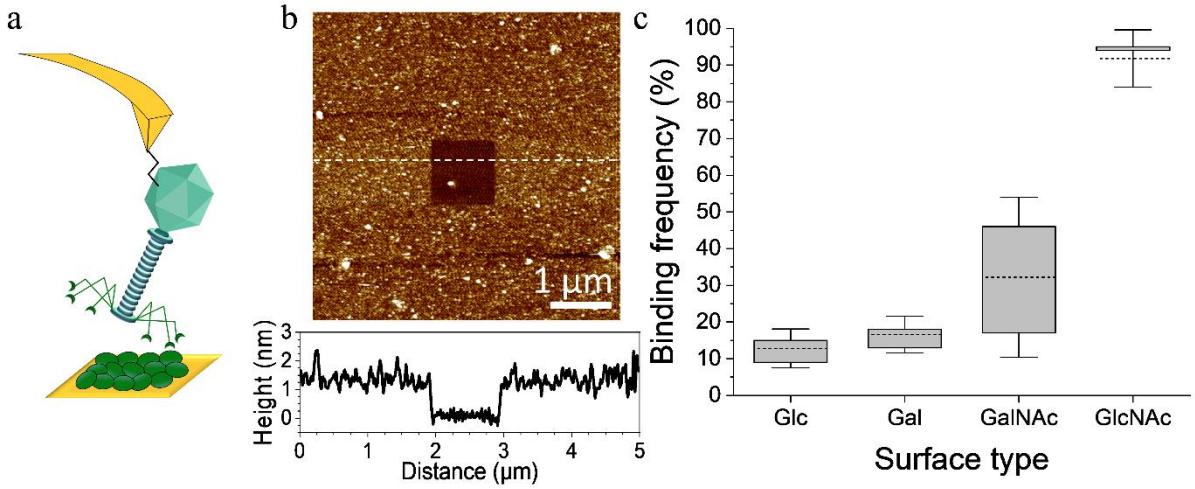

Figure 7. (a) AFM tips decorated with phage 187 were used to probe model surfaces coated monosaccharides. (b) Topography (AFM height image; 5 x 5 µm²; z scale = 6 nm) of GlcNAc coated substrates revealing a smooth and homogeneous surface. A vertical cross section taken along the dashed line is shown below the image. The thickness (~1.3 nm) was determined by imaging a square area of 1 x 1 µm² at large forces (>10 nN) before imaging 5 x 5 µm² of the same area at small forces. No scratches were observed for uncoated control surfaces. (c) Boxplot of adhesion frequencies of phage 187-decorated AFM tips on surfaces coated with monosaccharides. Boxes correspond to 25-75 percentiles, dashed lines to means and whiskers to standard deviations. Data were obtained from two independent experiments using different tips and surfaces.

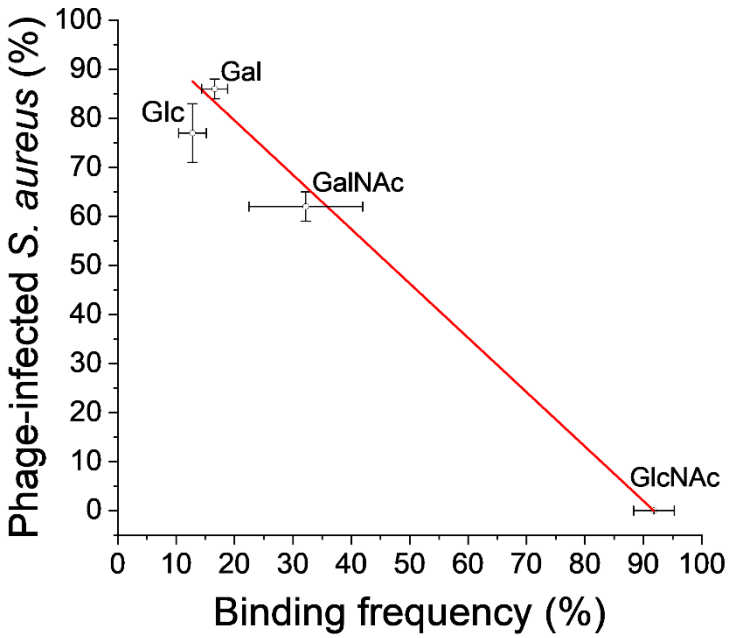

498

499 **Figure 8.** Correlation between the percentage of infected cells in presence of different free
500 monosaccharides and the adhesion frequency of phages towards surfaces coated with monosaccharides
501 (mean ± s.e.). The red line corresponds to a linear fit for eye guidance.

502